PHYSICAL REVIEW A **85**, 041801(R) (2012)

Probing the ladder of dressed states and nonclassical light generation in quantum-dot–cavity QED

Arka Majumdar,[*,†] Michal Bajcsy,[*,‡] and Jelena Vučković
E. L. Ginzton Laboratory, Stanford University, Stanford, California 94305, USA
(Received 9 June 2011; revised manuscript received 9 September 2011; published 12 April 2012)

We investigate the photon-induced tunneling phenomena in a photonic crystal cavity containing a strongly coupled quantum dot and describe how this tunneling can be used to generate photon states consisting mainly of a particular Fock state. Additionally, we study experimentally the second-order autocorrelation $g^2(0)$ in the photon-induced tunneling regime as a function of the frequency and the power of the probe laser and observe signs of higher manifolds of the Jaynes-Cummings Hamiltonian in the frequency-dependent photon statistics of the transmitted light, as well as the strong power dependence of $g^2(0)$, distinguishing this effect clearly from bunching occurring in a thermal light source.

DOI: 10.1103/PhysRevA.85.041801 PACS number(s): 42.50.Ar, 42.50.Ct, 42.50.Pq

A single-optical mode confined inside an optical cavity behaves like a simple harmonic oscillator, where all the energy levels are equally spaced. When this cavity mode is strongly coupled to a two-level quantum emitter such as a quantum dot (QD), the energy structure of the coupled system becomes anharmonic. This anharmonic (Jaynes-Cummings) ladder has been recently probed in atomic [1] and superconducting [2] cavity quantum electrodynamics (cQED) systems. Nonclassical correlations between photons transmitted through the cavity can result from such anharmonicity, which in turn leads to fundamental phenomena of photon blockade and photon-induced tunneling. These effects have been recently demonstrated in atomic systems [3], as well as in the solid-state platform [4]. Moreover, photon blockade and photon-induced tunneling can be used for applications beyond cQED, including the generation of single photons on demand [5] for quantum information processing, high precision sensing and metrology [6], as well as quantum simulation of complex many-body systems [7]. In this Rapid Communication, we explore the utility of the photon-induced tunneling and blockade for nonclassical light generation and probing of higher-order dressed states in the solid-state cQED system consisting of a single QD coupled to a photonic crystal cavity. First, we provide numerical simulation data showing that photon-induced tunneling can be used to preferentially generate specific multiphoton states. Following this, we present experimental data demonstrating the transition from a blockade to tunneling regime in such a system and show the signature of higher-order dressed states observed in the measured photon statistics. The probing of the ladder of dressed states by photon-correlation measurement has previously been performed experimentally only in an atomic cavity QED system [1], while in solid-state systems it has been studied theoretically [8] and signatures of higher-order dressed states were observed only using four wave mixing [9].

The dynamics of a coupled QD-cavity system, coherently driven by a laser field [Fig. 1(a)], is well described by the Jaynes-Cummings Hamiltonian of the form

$$H = \Delta_a \sigma_+ \sigma_- + \Delta_c a^\dagger a + g(a^\dagger \sigma_- + a\sigma_+) + \mathcal{E}(t)(a + a^\dagger), \tag{1}$$

which assumes the rotating wave approximation (RWA) and a frame of reference rotating with the frequency of the laser field ω_l. Here $\Delta_a = \omega_a - \omega_l$ and $\Delta_c = \omega_c - \omega_l$ are, respectively, the detunings of the laser from the QD resonant frequency ω_a and from the cavity resonance frequency ω_c, g is the coherent coupling strength between the QD and the cavity mode, $\mathcal{E}(t) = \sqrt{\frac{\kappa P(t)}{2\hbar\omega_c}}$ [10] is the slowly varying envelope of the coherent driving field with power $P(t)$ incident onto the cavity with field decay rate κ, and a is the annihilation operator for the cavity mode. If the excited and ground states of the QD are denoted by $|e\rangle$ and $|g\rangle$ then $\sigma_- = |g\rangle\langle e|$ and $\sigma_+ = |e\rangle\langle g|$. Two main loss mechanisms in this system are the cavity field decay rate $\kappa = \omega_c/2Q$ (Q is the quality factor of the resonator) and QD spontaneous emission rate γ. When the coupling strength g is greater than $\frac{\kappa}{2}$ and γ, the system is in the strong coupling regime [11–13]. In this regime, energy eigenstates are grouped in two-level manifolds with eigenenergies given by $n\omega_c \pm g\sqrt{n}$ (for $\omega_a = \omega_c$), where n is the number of energy quanta in the coupled QD cavity system [Fig. 1(b)]. The eigenstates can be written as

$$|n,\pm\rangle = \frac{|g,n\rangle \pm |e,n-1\rangle}{\sqrt{2}}. \tag{2}$$

Signatures of the photon blockade and tunneling can be detected through photon-statistics measurements, such as the second-order coherence function at time delay zero $g^{(2)}(0) = \frac{\langle a^\dagger a^\dagger a a\rangle}{\langle a^\dagger a\rangle^2}$. $g^{(2)}(0)$ is less (greater) than 1 in the photon blockade (tunneling) regime, signifying the presence of single (multiple) photons in the light coming out of the coupled QD cavity system. $g^{(2)}(0)$ can be experimentally measured by the Hanbury-Brown and Twiss (HBT) setup, where coincidences between the photons are detected [4]. Another important statistical quantity is the nth order differential correlation function $C^{(n)}(0) = \langle a^{\dagger n} a^n\rangle - \langle a^\dagger a\rangle^n$, which provides a clearer measure of the probability to create n photons at once in the cavity [1]. The second-order differential correlation function can also be expressed as $C^{(2)}(0) = [g^{(2)}(0) - 1]n_c^2$, where $n_c = \langle a^\dagger a\rangle$ is the average intracavity photon number. Particularly for

*Equal Contributors:
†arkam@stanford.edu
‡bajcsy@stanford.edu

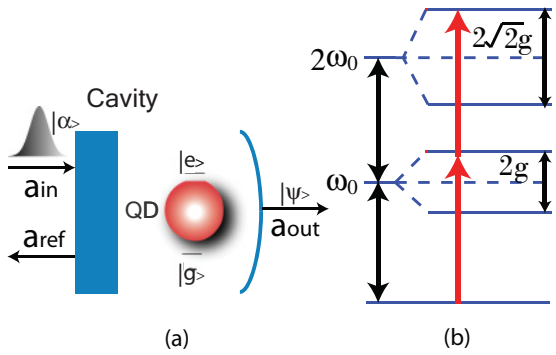

FIG. 1. (Color online) (a) Schematic of the coupled QD-cavity system driven by a Gaussian pulse (coherent state $|\alpha\rangle$). The transmitted light through the cavity is nonclassical ($|\psi\rangle$) due to the nonlinearity provided by the strongly coupled QD-cavity system. (b) The anharmonic Jaynes-Cummings ladder structure.

a weakly driven system ($n_c \ll 1$), $C^{(2)}(0)$ becomes positive only when the probability of the two-photon state becomes significant compared to that of a single-photon state, while a peak in $C^{(2)}(0)$ indicates the maximum probability of a two-photon state inside the cavity. As the driving power increases, the peak in $C^{(2)}(0)$ shifts toward empty cavity resonance as one starts populating the higher-order manifolds. This is described below and in the supplementary material.

Although the photon blockade and tunneling phenomena can be observed under continuous wave (CW) excitation in a numerical simulation [10], for practical consideration it is important to analyze the response of the cavity-QD system to a pulsed driving field. In particular, the ability to measure the photon statistics of the system's output during the actual experiment is determined by the time resolution capabilities of the single photon counters in the HBT setup, which in practice do not allow for the $g^{(2)}$ measurement of a CW-driven cavity-QD system. A common way to overcome this limitation is to drive the strongly coupled cavity-QD system with a train of weak, coherent pulses of sufficiently narrow bandwidth [4]. We use the quantum trajectory method [14,15] to analyze the pulsed driving of the coupled QD-cavity system and find the resulting photon statistics [5]. We also investigate the effect of pure QD dephasing [16] on the photon statistics and observe that, even though the actual value of $g^{(2)}(0)$ is affected due to dephasing, the qualitative nature of the $g^{(2)}(0)$ spectrum remains the same [10]. As the nonclassical state is collected from the cavity, only the collapse operator corresponding to the cavity decay (a) is monitored. A histogram is calculated based on the photon counts in the cavity decay channel and probability $P(n)$ for having exactly n photons in the system is found. The driving term $\mathcal{E}(t)$ in the Hamiltonian described in Eq. (1) is assumed to be of the form $\mathcal{E}(t) = \mathcal{E}_o \exp(-\frac{t^2}{2\tau_p^2})$, where $\mathcal{E}_o$ is the peak amplitude of the pulse. We set $\tau_p =$ 24.4 ps [i.e., full width at half maximum (FWHM) of 34 ps], which satisfies the narrow-band condition and corresponds to our experimental parameters.

Figure 2 shows the behavior of the system with better than current state of the art [17], but achievable experimental parameters [assuming the QD dipole moment of 30 Debye embedded in a linear three-holes defect cavity with mode

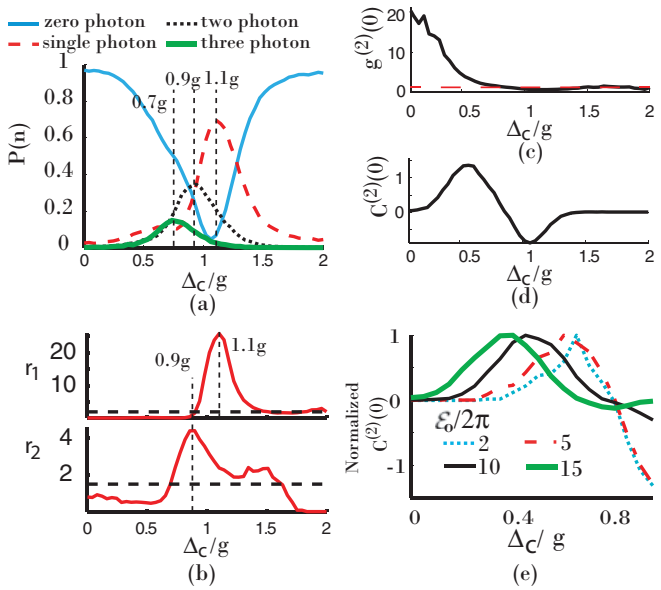

FIG. 2. (Color online) Numerically calculated photon statistics at the output of the QD-cavity system driven by Gaussian pulses with duration $\tau_p \sim 24$ ps. The simulation parameters are $g = 2\pi \times$ 40 GHz, $\kappa = 2\pi \times 4$ GHz, and $\mathcal{E}_o = 2\pi \times 9$ GHz; pure QD dephasing is neglected. (a) $P(n)$, probability of generating an n photon state at the cQED system output as a function of laser-cavity detuning Δ_c. (b) The ratios r_1 and r_2 (see text for details) as a function of Δ_c. $r_m = \frac{P(m)^2}{P(m-1)P(m+1)}$, where $P(m)$ is the probability of having m photons in the light. The dotted lines show the expected values of the ratios from a classical coherent state. (c) Second-order autocorrelation $g^{(2)}(0)$ as a function of Δ_c. The red dashed line shows the expected $g^{(2)}(0)$ for a coherent state. (d) Second-order differential correlation $C^{(2)}(0)$ as a function of Δ_c. (e) $C^{(2)}(0)$ as a function of the laser-cavity detuning Δ_c for different values of the peak laser field $\mathcal{E}_o/2\pi$ (in units of GHz). Every plot is normalized by the maximum $C^{(2)}(0)$, so that the peak value becomes 1 for all the plots. We observe that the peak in the $C^{(2)}(0)$ occurs at $\Delta_c = 0.7g$ for weaker excitation (where the second-order manifold is excited resonantly via two photons). However, with increasing excitation power, the peak positions shifts toward $\Delta_c = 0$ due to excitation of higher manifolds.

volume $\sim 0.7(\lambda/n)^3$] resulting in $g = 2\pi \times 40$ GHz and $\kappa = 2\pi \times 4$ GHz. These parameters can be achieved by improving the alignment of the QD to the cavity field and optimizing the photonic crystal cavity fabrication process to achieve a higher-quality factor. The results in Fig. 2(a) show that such a cavity-QD system can be employed to deterministically and preferentially generate a nonclassical state with a high fraction of a particular Fock state inside the cavity (no pure QD dephasing is included in the simulation). The detuning values ($1.1g$, $0.9g$, and $0.7g$) are different from what one intuitively expects from a lossless strongly coupled QD-cavity system under CW driving (g, $g/\sqrt{2}$, and $g/\sqrt{3}$, corresponding to the excitation of first-, second-, and third-order manifolds, respectively) because of both the losses and the pulsed driving of the system [4]. We note that, in the presence of pure QD dephasing, $P(n)$ for n photon states decreases [10]. We also note that even for a coherent state $|\alpha\rangle = \sum_n \frac{\alpha^n}{\sqrt{n!}}|n\rangle$, it is possible to have a particular Fock state $|m\rangle$ to be the state with the highest probability $P(m)$ of occurrence by choosing

α such that $m+1 > \alpha^2 > m$. However, for a coherent state the ratio $r_m = \frac{P(m)^2}{P(m-1)P(m+1)} = 1 + 1/m$ does not depend on α, and that cannot be increased by changing power in the coherent state. However, using the strongly coupled QD-cavity system, one can preferentially generate Fock states with probabilities that exceed this classical ratio achievable in a coherent state. This is shown in Fig. 2(b), where we compare the ratio r_m for 1 and 2 photon Fock state for a classical coherent state and the nonclassical state generated by the coupled QD-cavity system. We clearly see a large increase in the ratio $r_1(r_2)$ for the QD-cavity system at a detuning $\sim 1.1g$ ($\sim 0.9g$) showing that at those detunings we are preferentially generating 1 and 2 photon Fock states.

From the probability distribution of the different Fock states we can find the wave function of the overall photon state $|\psi\rangle = \sum_n c_n|n\rangle$ with $P(n) = |c_n|^2$, the second-order coherence function $g^{(2)}(0) = \langle\psi|a^\dagger a^\dagger aa|\psi\rangle/\langle\psi|a^\dagger a|\psi\rangle^2 = (\sum_n n(n-1)P(n))[\sum_n nP(n)]^2$, and second-order differential correlation function $C^{(2)}(0) = \langle\psi|a^\dagger a^\dagger aa|\psi\rangle - \langle\psi|a^\dagger a|\psi\rangle^2 = \sum_n n(n-1)P(n) - (\sum_n nP(n))^2$, which we can measure experimentally. Figure 2(c) shows $g^{(2)}(0)$ as a function of Δ_c, the laser detuning from the empty cavity. The dashed line indicates the expected $g^{(2)}(0)$ for a coherent state. Figure 2(d) shows $C^{(2)}(0)$ as a function of Δ_c. $C^{(2)}(0)$ transitions from a negative to positive value with decreased detuning at $\Delta_c \sim 0.9g$ thanks to the excitation of the second manifold in the ladder when two photons are simultaneously coupled into the cavity-QD system. Figure 2(e) shows $C^{(2)}(0)$ as a function of Δ_c for different laser excitation powers. We note that the peak position changes depending on the excitation laser power and at lower driving power we observe the peak at $\Delta_c \sim 0.7g$, where the second-order manifold is excited via two photons. With increasing power, the higher (third and more) manifolds start being populated, and the peak in $C^{(2)}(0)$ subsequently shifts to smaller values of detuning. In Fig. 2(d), the peak in $C^{(2)}(0)$ is at a detuning of $\Delta_c \sim 0.5g$.

We confirm our theoretical predictions by performing an experiment with InAs QDs coupled to a linear three-hole defect GaAs photonic crystal cavity. Details of the fabrication and experimental setup can be found in Ref. [4]. We measure laser transmission through the system (using a cross-polarized reflectivity setup [4]) and observe anticrossing between the QD and cavity (by changing temperature) signifying the system is in the strong coupling regime. At resonance, the QD and cavity mix to generate two polaritons, seen as two Lorentzian peaks in Fig. 3(a). By fitting the spectrum at resonance we estimate the system parameters as $\kappa/2\pi = 27$ GHz (corresponding to $Q \approx 6000$) and $g/2\pi = 21$ GHz. To drive the cavity-QD system, we use a mode-locked Ti-sapphire laser that generates 3 ps pulses at a repetition rate of $f_{\text{rep}} = 80$ MHz. These 3 ps pulses are passed through a monochromator to elongate the pulse in time domain, which results in pulses with approximately Gaussian temporal profile of 34 ps FWHM, corresponding to $\tau_p = 24.44$ ps (as in our theoretical analysis). We determine the amplitude of the coherent driving field using $\mathcal{E}_o = \sqrt{\frac{\eta P_{\text{avg}}}{4\pi \frac{1}{2} Q\tau_p f_{\text{rep}}\hbar}}$ (see the supplementary material), where P_{avg} is the average optical power of the pulse train measured before the objective lens and $\eta \sim 0.03$ [4] is the coupling efficiency of the incident

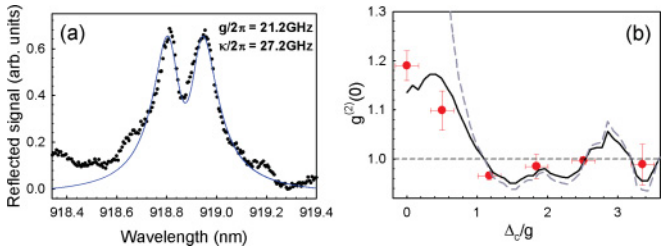

FIG. 3. (Color online) (a) The transmission spectrum of a strongly coupled QD-cavity system showing two polaritons. (b) Second-order coherence function at $t = 0$, $g^{(2)}(0)$ as a function of the laser detuning from the empty cavity frequency. The system is excited with $\tau_p = 24$ ps Gaussian pulses, with 80 MHz repetition frequency. The dashed gray (solid black) line results from a numerical simulation based on the system's experimental parameters and no (with) QD blinking. The average laser power for the measurement is $P_{\text{avg}} = 0.2$ nW. For the simulations we use a QD dephasing rate $\gamma_d/2\pi = 1$ GHz.

light into the cavity including all the optics losses. For our experimental parameters, $\mathcal{E}_o \approx 2\pi\sqrt{P_{\text{avg}}(nW)} \times 9.3$ GHz. The second-order autocorrelation $g^{(2)}(0)$ is measured as a function of excitation laser frequency [Fig. 3(b)] to observe the transition from photon blockade to photon-induced tunneling regime. The measurement setup has a timing resolution of 100 ps. Typical histograms obtained for blockade and tunneling are shown in the supplementary material. We estimate $g^{(2)}(0)$ as the ratio of the coincidence counts at zero time delay and at a time delay much larger than the time scale of the system dynamics (~ 1 ns).

Following this we calculate the second-order differential correlation function $C^{(2)}(0)$ for the coupled-QD cavity system as a function of the laser-cavity detuning [Fig. 4(a)]. We observe the transition of $C^{(2)}(0)$ from negative to positive values. Simulations with our system parameters are shown by the dashed line in Fig. 4(a) and the onset of a peak at $\Delta_c \sim 0.5g$ corresponding to the excitation of the higher-order dressed states is observed. The absence of such a clear peak in the experimental data can be ascribed to QD blinking. As explained before, the peak in $C^{(2)}(0)$ does not correspond exactly to the resonant excitation of the second-order manifold via the two-photon process because of the additional excitation of the higher-order manifolds. All the measurements are performed at 14 K. We note that, in the simulation, $g^{(2)}(0)$ in the tunneling regime is much larger than the experimentally measured value as a result of QD blinking, which causes the experimentally collected data to be a weighted average of transmission through an empty cavity and a cavity with strongly coupled QD; in other words, blinking effectively pulls the $g^{(2)}(0)$ curve toward $g^{(2)}(0) = 1$ [4]. We model the blinking behavior of the QD by assuming that during a unit time interval the QD is active for a fraction r and inactive for $(1-r)$ of the time. Thus the $g^{(2)}(0)$ measured in the experiment will be a statistical mixture of the coherent photon state (when QD is inactive, i.e., QD-cavity coupling $g = 0$) and the correlated photons from the coupled QD-cavity system [10]. We obtain a good fit to our experimental data with $r = 0.65$. The vertical error bars in all the figures are calculated from the uncertainties in the fit of the histogram data sets. The horizontal error bars

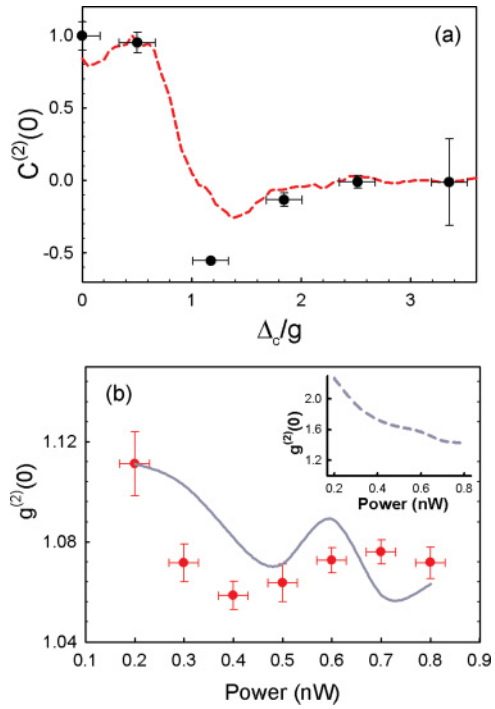

FIG. 4. (Color online) (a) Normalized differential correlation function $C^{(2)}(0)$ as a function of the laser detuning. The dashed red line shows the result of a numerical simulation based on the system's experimental parameters. (b) $g^{(2)}(0)$ in the tunneling regime ($\Delta_c = 0$) as a function of laser power P_{avg} measured in front of the objective lens. The solid line shows the result of numerical simulation including the effects of QD blinking, while the inset plots the numerically simulated $g^{(2)}(0)$ in the absence of blinking. For the simulations we use a QD dephasing rate $\gamma_d/2\pi = 1$ GHz.

are given by the uncertainty in the measurement of the laser wavelength or the laser power.

Finally, Fig. 4(b) shows $g^{(2)}(0)$ as a function of excitation laser power in the tunneling regime ($\Delta_c = 0$). These data are taken with the same cQED system on a different day, when the cavity is red-shifted compared to the previous measurements. For this particular experiment, the QD and the cavity are resonant at 26 K. This slightly higher temperature might cause more QD dephasing, leading to a worse value of $g^{(2)}(0)$ (1.12 as opposed to 1.2 from the previous measurement). Overall, $g^{(2)}(0)$ decreases with increasing laser power as expected from the intuitive picture of QD saturation at high driving power and the numerical simulation. This clearly shows that the photon bunching observed in the tunneling regime is coming solely from the quantum-mechanical nature of the QD-cavity system and not from a classical effect. We also observe an interesting oscillatory behavior in $g^{(2)}(0)$ as a function of power. An oscillatory behavior is also observed in the simulation that includes the effects of QD blinking. Without any QD blinking, the simulation results show a mostly monotonically decreasing $g^{(2)}(0)$ with increasing laser power [inset of Fig. 4(b)].

Finally, we would like to point out that these measurements have been performed at the lowest $P_{\text{avg}} = 0.2$ nW that we can reliably use, corresponding to $\mathcal{E}_o \approx 2\pi \times 4.2$ GHz. This roughly corresponds to the red plot in the theoretical Fig. 2(e), where the peak in $C^{(2)}(0)$ is near $\sim 0.5g$. This lower power limit is caused by the limited mechanical stability of the cryostat and the low overall efficiency with which we can couple the cavity photons into the single photon counters in our HBT setup. The time needed to perform the second-order coherence measurement increases quadratically with decreasing P_{avg} and for low powers the cavity drifts out of focus before we can collect sufficient number of coincidence counts.

In summary, we analyzed the photon-induced tunneling regime in a coupled QD-cavity system and proposed a scheme to use this system for multiphoton state generation. In addition, we experimentally characterized the second-order coherence function $g^{(2)}(0)$ for a coupled QD-cavity system as a function of laser-cavity detuning and laser power. Using the experimental results of the photon statistics measurement, we find signs of the higher-order manifolds of the Jaynes-Cummings anharmonic ladder in the second-order differential correlation function $C^{(2)}(0)$ and we confirm the quantum origin of the photo-induced tunneling effect.

The authors acknowledge financial support provided by DARPA, ONR, NSF, and the ARO and useful discussion with Dr. Andrei Faraon. The authors also acknowledge Dr. Pierre Petroff and Dr. Hyochul Kim for providing the QD sample.

[1] A. Kubanek *et al.*, Phys. Rev. Lett. **101**, 203602 (2008).
[2] Lev S. Bishop *et al.*, Nature Physics **5**, 105 (2009).
[3] K. M. Birnbaum *et al.*, Nature (London) **436**, 87 (2005).
[4] A. Faraon *et al.*, Nature Physics **4**, 859 (2008).
[5] A. Faraon, A. Majumdar, and J. Vuckovic, Phys. Rev. A **81**, 033838 (2010).
[6] I. Afek *et al.*, Science **32**, 879 (2010).
[7] I. Carusotto *et al.*, Phys. Rev. Lett. **103**, 033601 (2009).
[8] F. P. Laussy *et al.*, e-print arXiv:1104.3564v2.
[9] J. Kasprzak *et al.*, Nat. Mater. **9**, 304 (2010).
[10] See Supplemental Material at http://link.aps.org/supplemental/10.1103/PhysRevA.85.041801 for a detailed analysis of $C^2(0)$ both under pulsed and continuous wave excitations.
[11] T. Yoshie *et al.*, Nature (London) **432**, 200 (2004).
[12] E. Peter *et al.*, Phys. Rev. Lett. **95**, 067401 (2005).
[13] J. P. Reithmaier *et al.*, Nature (London) **432**, 197 (2004).
[14] *An Open Systems Approach to Quantum Optics*, edited by H. Carmichael (Springer, Berlin, 1993).
[15] H. Goto and K. Ichimura, Phys. Rev. A **72**, 054301 (2005).
[16] D. Englund *et al.*, Phys. Rev. Lett. **104**, 073904 (2010).
[17] A. Tandaechanurat *et al.*, Nature Photonics **5**, 91 (2011).